

1

# Accelerators and beam physics

# Observation of Intense Terahertz Synchrotron Radiation Produced by Laser Bunch Slicing at UVSOR-II

M. Shimada<sup>1</sup>, M. Katoh<sup>1,2</sup>, A. Mochihashi<sup>1</sup>, S. Kimura<sup>1</sup>, T. Hara<sup>1\*</sup>, M. Hosaka<sup>2</sup>, Y. Takashima<sup>2</sup>, T. Takahashi<sup>3</sup>

<sup>1</sup>*Institute for Molecular Science, Myodaiji-cho, Okazaki, 444-8585 Japan*

<sup>2</sup>*Nagoya University, Furo-cho, Chikusa-ku, 464-8603 Japan*

<sup>3</sup>*Kyoto University, Kumatori-cho, Sennan-gun, Osaka, 590-0494 Japan*

Coherent synchrotron radiation in terahertz region (THz CSR) can be produced from the sub-mm scale micro-structure on the longitudinal density distribution of the electron bunches. THz CSR is generated by the bunch instability [1] and the laser bunch slicing, which is a technique to produce the micro-structures on the electron bunches. In the laser bunch slicing, a femto-second ultra-short laser pulse interacts with an electron bunch in an undulator and induces the energy modulation in the bunch. As the bunch transports in the ring, the modulated electrons are separated from the bunch and a dip is created. We succeeded to observe high intensity THz CSR from the modulated electron bunch.

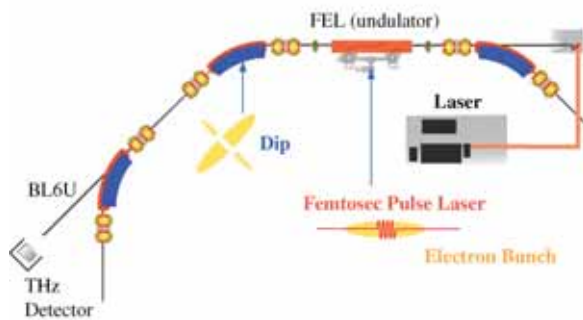


Fig. 1 Schematic of the laser bunch slicing system.

The laser system is composed of a mode-lock Ti:Sa laser and a regenerative amplifier as illustrated in Fig. 1. The former generates laser pulses synchronized with electron bunches and the latter generates intense ultra-short laser pulses with energy of 2.5 mJ/pulse and repetition rate of 1 kHz.

The laser pulses are introduced to the ring through a laser transport line conducted to the undulator in the free electron laser. The laser pulses and the electron bunches interact in the undulator polarized horizontally and tuned at the laser wavelength, 800 nm. The streak camera was used for spatial and temporal alignment between the laser beam and the electron beam.

The ring was operated in the single bunch mode at 600 MeV, which is suitable to tune the undulator at the laser wavelength, 800 nm. The THz CSR is observed at, BL6B, which is connected to the second bending magnet from the undulator section, and has a large solid angle, 215 mrad x 80 mrad [2]. The

collected THz CSR is introduced to a liquid He cooled InSb bolometer, which is sensitive to the wavelength region between 0.2 mm to 3.0mm.

Intensity of the terahertz pulses generated by the laser bunch slicing is  $10^4 - 10^5$  times higher than that of the normal synchrotron radiation. The detector output for the individual pulse of THz CSR is also shown in Fig.2. The pulse width is a few micro-second, which is almost the same as the temporal resolution of the bolometer.

The intensity of the pulse of THz CSR was plotted as a function of the beam current in Fig. 3. The intensity is proportional to square of the peak current of the electron beam which was obtained experimentally by using a streak camera. This result clearly indicates that the observed THz radiation is coherent.

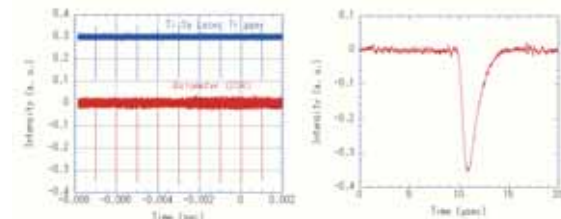


Fig. 2 (Left) terahertz pulses induced by the laser injection. (Right) detector output signal (negative) for individual terahertz pulse.

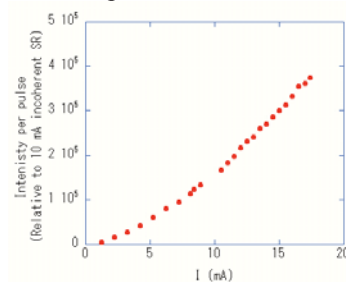


Fig. 3 Intensity of THz CSR versus peak current of electron bunch. The solid line is a best-fit square curve.

[1] Y. Takashima *et al.*, Jpn. J. Appl. Phys. **44** (2005) 1131.

[2] S. Kimura *et al.*, AIP Conf. Proc. **705** (2004) 416.

\*Guest associate professor from RIKEN/SPring-8

## Storage Ring FEL Exceeding 1 W in the Deep UV Region

M. Hosaka<sup>1</sup>, M. Katoh<sup>1,2</sup>, A. Mochihashi<sup>1</sup>, M. Shimada<sup>1</sup>, J. Yamazaki<sup>1</sup>, K. Hayashi<sup>1</sup>,  
Y. Takashima<sup>2</sup>

<sup>1</sup>*UVSOR Facility, Institute for Molecular Science, Okazaki 444-8585 Japan*

<sup>2</sup>*Department of Material Processing Engineering, Graduate School of Engineering, Nagoya University, Chikusa-ku, Nagoya 464-8603 Japan*

Thanks to a recent upgrade of the UVSOR-II storage ring (lower beam emittance and higher peak current), an FEL gain has been enhanced much and we have succeeded in high power lasing in deep UV region. In 2005 we replaced rf accelerating cavity system [1]. The aim is to improve lifetime of the electron beam with higher accelerating voltage. At the UVSOR, 90.1 MHz rf cavity had been operated with a 20 kW transmitter but the rf accelerating voltage (55 kV at maximum) was limited by low shunt impedance (1 M $\Omega$ ) of the former cavity. Hence the new rf cavity was designed to have higher shunt impedance. The new cavity was installed in the spring of 2005 and the high cavity voltage of 150 kV was achieved. This upgrade is favourable to the FEL because higher accelerating voltage leads to shorter electron bunch and higher peak current.

The lasing experiment around 230 nm was planned oriented to users experiment [2]. Multi-layers of Al<sub>2</sub>O<sub>3</sub>/SiO<sub>2</sub> were also employed for cavity mirrors. Measured round-trip reflectivity and transmission were 98.8 % and 0.8%, respectively. The lasing experiment was carried out with an electron energy of 750 MeV. Former UVSOR FEL experiment had been made with an electron energy of 600 MeV. Recently we raised the electron energy from 600 MeV to 750 MeV, with which the storage ring is operated for SR use. According to the Renieri limit [3], the extracted FEL power is proportional to the total synchrotron radiation power per turn from electron beam. Since the total radiation power is proportional to

the 4th power of the electron energy, higher extracted laser power is expected at 750 MeV. The measured threshold current for lasing is about 2 times higher than that in the case of 600 MeV. But a higher laser power is extracted. The observed maximum power reached 1.1 W at a beam current of 100 mA/bunch. During the experiment, drift of the laser power was observed especially at a high beam current as shown in the figure. The power could be recovered by adjusting the alignment with downstream mirror once again. Therefore the power drift can be explained by deformation of the cavity mirror due to heat-load from synchrotron radiation and from the FEL. The laser, however, became almost stable after about one hour exposure of synchrotron radiation. The FEL around 230 nm was applied to two experiments on surface physics and photo-electron spectroscopy. The FEL extracted from the upstream mirror was transported to the experimental stations by using aluminium mirrors and was focused on samples by lenses. In the experiments, they started the measurement after the laser became stable. The FEL power around 0.5 ~ 0.2 W was actually applied. Although the experiments were made in limited machine time, the users succeeded in obtaining primary results.

[1] A. Mochihashi *et al.*, UVSOR Activity Report 2005 (2006).

[2] T. Nakagawa *et al.*, UVSOR Activity Report 2006 (2007).

[3] A. Renieri, *Nuovo Cimento* **53** (1979) 160.

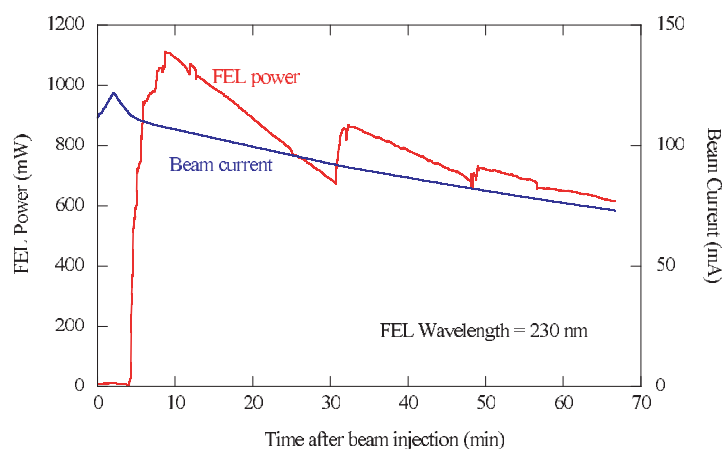


Fig. 1 Extracted FEL power and beam current as a function of time. The FEL wavelength is around 230 nm.

## Coherent Harmonic Generation Experiment

M. Labat<sup>1</sup>, G. Lambert<sup>1,2</sup>, M.E. Couprie<sup>3</sup>, Y. Takashima<sup>5</sup>, T. Hara<sup>4</sup>, M. Hosaka<sup>5</sup>, A. Mochihashi<sup>6</sup>, J. Yamazaki<sup>6</sup>, M. Shimada<sup>6</sup>, M. Katoh<sup>6</sup>

<sup>1</sup>CEA Saclay, 91 191 Gif-sur-Yvette France

<sup>2</sup>Synchrotron Soleil, Saint Aubin France

<sup>3</sup>Laboratoire Aimé Cotton, Orsay France

<sup>4</sup>RIKEN SPring-8 Harima, Hyogo Japan

<sup>5</sup>Nagoya University, Nagoya Japan

<sup>6</sup>UVSOR Facility, Institute for Molecular Science, Okazaki 444-8585 Japan

Coherent Harmonic Generation (CHG) is a seeded Free Electron Laser configuration based on storage ring [1]. A Ti:Sa laser is focused in the first part of the optical klystron (OK): the modulator, and synchronized with the circulating electron bunch. The electron beam is micro bunched at fundamental and sub harmonic wavelengths of the seeded laser. The light emission of the electrons is then enhanced in the second OK part, the radiator, at the third harmonic of the seed, i.e. 266 nm.

The intensity of the light emitted by a relativistic electron bunch in an optical klystron can be expressed as the sum of an incoherent and a coherent term. The coherent term equals zero for randomly distributed electronic phases. In the case of CHG process, the interaction between the electric field and the electrons induces a modulation of the distribution: the intensity of the coherent emission no longer averages to zero.

For CHG experiment, the machine is operated at 600 MeV in single bunch mode. The modulator and radiator of the BL5U OK are identical and separated by a dispersive section. The detection of the UV light is performed using a solar blind PhotoMultiplier. In order to observe the coherent emission at 1 kHz, among incoherent emission at 5.6 MHz, its signal is observed on an oscilloscope, triggered by the laser timing system. A streak camera (Hamamatsu, C5680) allows following the longitudinal distribution of the electron bunch. The seeding laser is high repetition rate (1 kHz), short pulse duration (150 fs to 1 ps) Ti:Sa with 800 nm wavelength.

The temporal overlap in the modulator for the micro bunching of the electronic distribution requires a precise synchronization of the laser pulse and the electron bunch, using a specific timing system. The condition of synchronization is observed with the streak camera, which temporal resolution reaches 10 ps. Spatial overlap is obtained adjusting the laser path on the electron orbit.

A picture of the PM signal is presented in Figure 1, illustrating the output radiation of the undulators. Central peak corresponds to the radiation of the laser heated electron bunch. The intensity at 266 nm is dramatically enhanced thanks to the coherent emission at the third harmonic of the seeding laser.



Fig. 1 Oscilloscope trace of the optical klystron out put radiation. Laser power=1.78 W, I=4.29mA. Time scale: 40 ns/division.

Figure 2 shows the streak camera image of CHG signal. This diagnostic confirms the enhancement of the intensity at 266 nm radiated by the heated electron bunches (see bright blue spots).

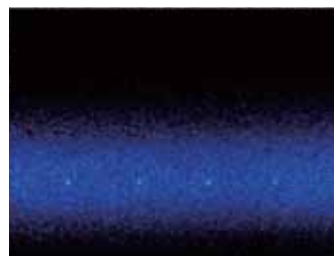


Fig. 2 Photograph of the streak camera image. Full scales are 85 ms for the horizontal and 700 ps for the vertical axis.

First results confirmed the expected quadratic dependency of the coherent emission with peak current. An optimum undulator gap for CHG emission was found at 40.8 mm and the signal vanishes for gaps below 39.7 and over 42.5 mm.

Using a 1 kHz Ti:Sa laser, a Coherent Harmonic Generation FEL configuration has been successfully set up at UVSOR-II facility. Short (below 2 ps), UV (266 nm), coherent laser pulses are delivered.

[1] R. Prazeres, J.M. Ortega, C. Bazin, M. Bergher, M. Billardon, M.E. Couprie, M. Velgue and Y. Petroff, Nucl. Inst. Meth. A **272** (1988) 68-72.

## Variation of Circumference of UVSOR-II

K. Suzumura<sup>1</sup>, M. Katoh<sup>2,1</sup>, Y. Takashima<sup>1</sup>, K. Hayashi<sup>2</sup>, A. Mochihashi<sup>2</sup>, J. Yamazaki<sup>2</sup>, M. Hosaka<sup>1</sup>, M. Shimada<sup>2</sup>

<sup>1</sup>Graduate School of Engineering, Nagoya University, Chikusa-ku Nagoya 464-8603 Japan  
<sup>2</sup>UVSOR Facility, Institute for Molecular Science, Okazaki 444-8585 Japan

A drift of the electron orbit in a synchrotron light source causes a drift of the light source position, which makes harmful effects on the users experiments. Recently, we have developed a RF-FB system, to suppress orbit drift at UVSOR-II [1]. The system corrects automatically the drift by controlling the RF frequency, and its value is recorded during user operations. The system has been working successfully for about one year. By using the accumulated data, we can see the variation of the circumference of UVSOR-II in various time scales.

UVSOR-II is operated for users from Tuesday to Friday in a week, and from AM9:00 ~ PM9:00 in a day. Fig.1 shows variations of the RF frequency and of the floor temperature of the storage ring room during a week. During one day, the RF frequency decreases with time. The variation amplitudes during each day are about the same, but the absolute value decreases gradually throughout a week. On the other hand, the floor temperature increases with time during a day, and the absolute value increases throughout a week. As shown in Fig.1, the RF frequency shows strong correlation with the floor temperature. Fig.2 shows the variation of the RF frequency and the floor temperature during a year. The RF frequency varies through a year. It is higher in winter and lower in summer. The floor temperature also varies through a year. However, there can be seen no clear correlation with the RF frequency.

There can be seen a strong correlation between the RF frequency and the floor temperature during a day or during a week. This fact suggests that the variation of the circumference of the storage ring is mainly caused by thermal expansion of the floor. Because the storage ring components, such as magnets, are fixed rigidly to the floor, it is considered that the storage ring expands outward when the floor expands as its temperature increases.

We can quantitatively validate the assumption by comparing measured and theoretical values of the RF frequency using the measured floor temperature. The theoretical value can be calculated as following,

$$\Delta f_{RF} = -f_{RF} \cdot \alpha \cdot \Delta t,$$

where  $f_{RF}$  the RF frequency,  $\alpha$  the thermal expansion coefficient of the floor, and  $\Delta t$  the measured floor temperature variation. Each value is as following,  $f_{RF}=90.1\text{MHz}$ ,  $\alpha=1.0 \times 10^{-5}/^\circ\text{C}$  for concrete and  $\Delta t=0.8^\circ\text{C}$  in a day. As assigning these values to the expression, the theoretical value of  $\Delta f_{RF}$  in a day becomes 0.72kHz. As shown fig.1, the measured value in a day is about 0.6kHz. The theoretical value

is close to the actual measurement value. From this result, there is a high possibility that the main cause of the variation of the circumference is the thermal expansion of the floor.

It seems that there is no clear correlation between  $f_{RF}$  and  $\Delta t$  through a year, as shown in Fig. 2. However, it seems to have good correlation with the outdoor temperature. This point may be discussed after several year operation of the RF-FB system.

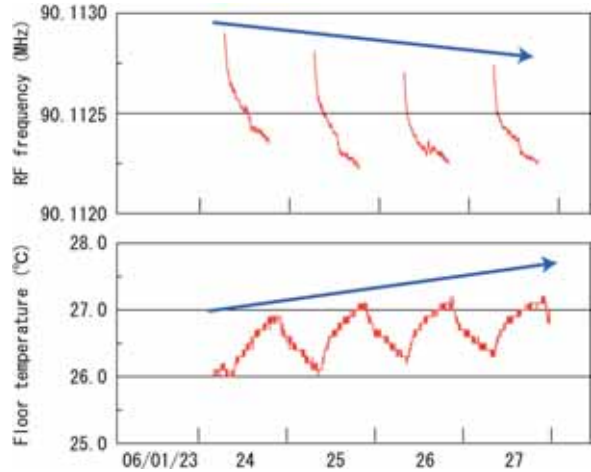


Fig.1 The variation of RF frequency and floor temperature of a week.

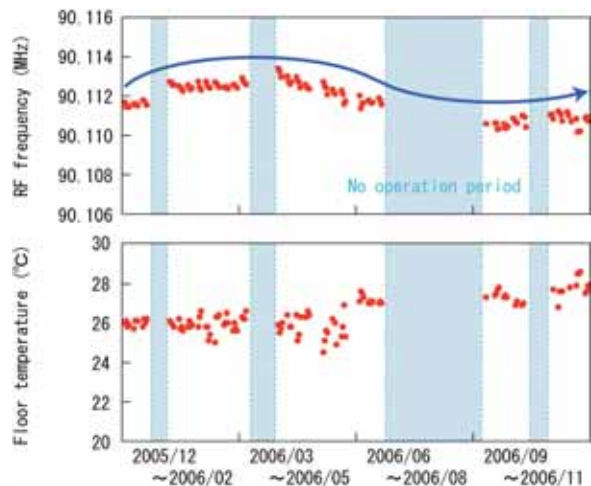


Fig.2 The variation of RF frequency and floor temperature of a year.

[1] K. Suzumura *et al.*, UVSOR Activity Report 2005 (2006), 39

## Development of a BPM Displacement Measurement System at UVSOR-II

K. Suzumura<sup>1</sup>, M. Katoh<sup>2,1</sup>, Y. Takashima<sup>1</sup>, K. Hayashi<sup>2</sup>, A. Mochihashi<sup>2</sup>, J. Yamazaki<sup>2</sup>, M. Hosaka<sup>1</sup>, M. Shimada<sup>2</sup>

<sup>1</sup>Graduate School of Engineering, Nagoya University, Chikusa-ku Nagoya 464-8603 Japan  
<sup>2</sup>UVSOR Facility, Institute for Molecular Science, Okazaki 444-8585 Japan

The electron beam orbit of the UVSOR-II storage ring is measured by 24 BPMs (Beam Position Monitors), which are integrated on the beam ducts. Each BPM head consists of 4 electrodes, and detects the orbit by comparing the induced electric voltages on the electrodes. The data are used to correct the orbit. However, there is a possibility of measurement error caused by mechanical displacements of the BPM heads. We have developed a system to measure BPM displacement in real time.

The system we have developed is schematically shown in Fig.1. It consists of linear gauges, gauge counter, fixing clamps and PC for data logging. The read-out resolution of the linear gauges is one micron. The material of the fixing clamps is aluminum. They are fixed to iron cores of the bending magnet. With one fixing clamp, two linear gauges can be set to measure horizontal and vertical displacements at once. The data acquisition system on PC is developed by using LabVIEW7.0. The data are stored every 5 seconds.

The temperature of the storage ring room changes with time, because of the heats produced by the accelerator components, such as electric power supplies. We expected that the possibility of thermal deformation of the fixing jigs may cause measurement errors. We artificially changed the temperature of a jig using a heater, to see the effect of the thermal deformation. In the result, the error caused by the thermal deformation was less than ten microns for the temperature change in daily operation. So we disregard it in this research.

We measured BPM displacements during user operations. Fig.2 shows the BPM displacement and the orbit position measured at a BPM called No.2 during a user operation. At this BPM, the beam position shows a large motion of a few hundred microns. However, the BPM position also shows quite similar motion. These data indicate that the beam position does not move but the BPM moves. In fact, the beam duct on which the BPM No.2 is installed has a trouble on the cooling water channel. The temperature of the beam duct is changed by the irradiation of SR light, as shown in Fig.3. BPM No.1 is installed on the same beam duct and its position shows similar motion.

Fig.4 shows a BPM displacement and a beam position at another BPM, called No.11. The BPM displacement is much smaller than that of BPM No.2. But, still we observed some displacement of a few 10 microns. The beam position movement is much larger than this. Thus, we can say that this orbit movement

is real. It is similar at the other BPM on the beam ducts without water cooling trouble. However, when we try to stabilize the orbit movement less than 10 microns, we must consider the displacements of the BPMs. This measurement system will be integrated in the orbit correction system.

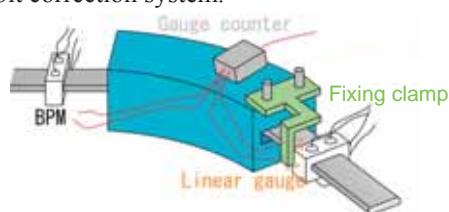


Fig.1 Schematic drawing of a BPM displacement measurement system.

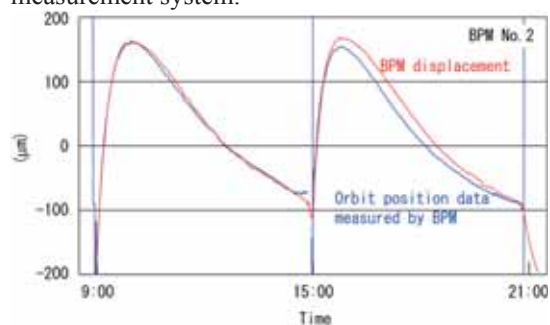


Fig.2 BPM displacement and orbit data measured by BPM during a user operation day at BPM2.

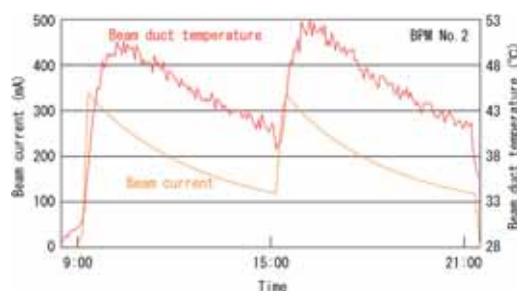


Fig.3 Beam current and beam duct temperature during a user operation day at BPM2.

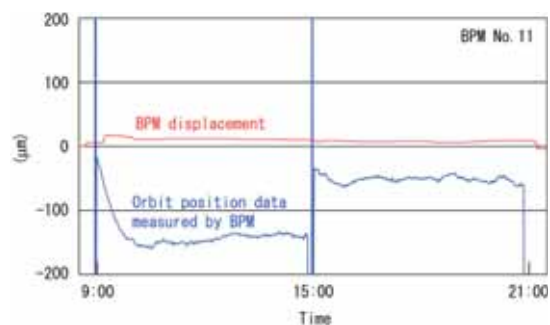


Fig.4 BPM displacement and orbit data measured by BPM during a user operation day at BPM11.

# Touschek Lifetime Measurement with a Spurious Bunch in Single-bunch Operation in UVSOR-II Electron Storage Ring

A. Mochihashi<sup>1</sup>, M. Katoh<sup>1,2</sup>, M. Hosaka<sup>2</sup>, Y. Takashima<sup>2</sup>, Y. Hori<sup>3</sup>

<sup>1</sup>UVSOR Facility, Institute for Molecular Science, Okazaki 444-8585 Japan

<sup>2</sup>Graduate School of Engineering, Nagoya University, Chikusa, Nagoya 464-8603 Japan

<sup>3</sup>High Energy Accelerator Research Organization (KEK) Oho, Tsukuba 305-0801 Japan

We have developed a method to measure the Touschek beam lifetime of an electron storage ring using spurious bunches in single-bunch operation by measuring changes in the single-bunch impurity over time. To measure a spurious bunch and the main bunch simultaneously, we use a photon counting method with sufficient dynamic range and response time. We demonstrate the method by measuring the Touschek beam lifetime in the UVSOR-II electron storage ring. We find that the Touschek beam lifetime dominates the total beam lifetime in UVSOR-II in the usual vacuum condition. In SuperACO[1], a method to measure the Touschek lifetime by storing two bunches whose intensities are different has been developed. The ‘two unequal bunches method’ is very effective for measuring the Touschek lifetime if it is assumed that the Touschek lifetime is inversely proportional to the number of electrons in the bunch. The need for the assumption can be avoided by preparing two bunches with extremely different bunch charges. If the Touschek lifetime of the weaker bunch of the two is very long compared with that of the more intense bunch, it is possible to measure the Touschek lifetime of the intense bunch without making any assumption about the dependence of the Touschek lifetime on the bunch charge. However, it is difficult to make two bunches that have extremely different bunch charges when the bunch charge of the intense bunch is small. To make two bunches with extremely different bunch charges, with the more intense bunch having a small bunch charge, use can be made of the phenomenon in which extremely weak bunches compared with the main bunch can be generated automatically in single-bunch operation in electron storage rings [2,3]. The spurious bunch charge is extremely small compared with the main bunch regardless of the size of the main bunch charge, and can be generated automatically. Even though a spurious bunch can grow continuously during a measurement, it is possible to cancel the effects of the growth and measure the Touschek lifetime of the main bunch precisely using only the intensity of the main and spurious bunches, without requiring calculated beam or storage ring parameters. We consider the change with time in the number of electrons in a main bunch  $N_0$  and that in the RF bucket immediately following the main bucket  $N_1$ . We assume the Touschek lifetime of the spurious bunch is much longer than that of the main bunch because of  $N_0 \gg N_1$ . When the growth of the spurious bunch in one Touschek lifetime period of the main bunch  $\tau_T(N_0)$  can be neglected compared with the

single-bunch impurity  $N_1/N_0$  the Touschek lifetime of the main bunch can simply be written as [4]

$$\frac{1}{\tau_T(N_0)} = \frac{d}{dt} \log \left( \frac{N_1}{N_0} \right). \quad (1)$$

If the assumption for the growth rate of the spurious bunch is not valid, it is still possible to measure the Touschek lifetime by repeating the measurement with a different spurious bunch charge with the same main bunch charge. For spurious bunch charges  $N_1$  and  $N_1^*$  ( $N_1 > N_1^*$ ) and main bunch charge  $N_0$ ,  $\tau_T(N_0)$  can also be written simply as

$$\frac{1}{\tau_T(N_0)} = \frac{d}{dt} \log \left( \frac{N_1 - N_1^*}{N_0} \right). \quad (2)$$

By considering the single-bunch impurity value in UVSOR-II, we adopted Eq.(2) to measure the Touschek lifetime in UVSOR-II. Figure 1 shows measured decay-rate and the Touschek beam lifetime in normal and poor vacuum conditions. To make the poor vacuum condition we turned off all of the ion pumps and heated a part of the beam ducts of the storage ring. In the figure, the decay-rate lifetime decreased in the poor vacuum condition but the Touschek lifetime still kept the same value as the normal vacuum condition. The vacuum pressure estimated from the beam lifetime agreed with the result from the vacuum gauge measurement.

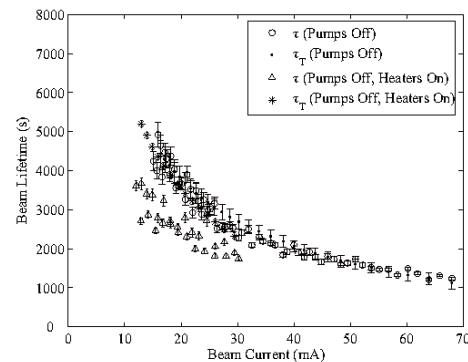


Fig.1 Measured decay-rate and Touschek lifetime in normal/poor vacuum condition in single-bunch operation.

- [1] J. C. Besson *et al.*, Commissioning of SuperACO, ORSAY Report RT-88-01,(1988) 34.
- [2] T. Kasuga *et al.*, Jpn. J. Appl. Phys. **28**(1989) 541.
- [3] T. Obina *et al.*, Nucl. Instrum. Methods Phys. Res. A **354** (1995) 204.
- [4] A. Mochihashi *et al.*, Nucl. Instrum. Methods Phys. Res. A **572** (2007) 1033.